Diode Laser Wavelength Tracking Using an Integrated Dual Slab Waveguide Interferometer

Graham H. Cross and Ellen E. Strachan

***Abstract*—The problem of tracking small changes in the output wavelength of laser diodes is addressed using a dual slab waveguide interferometer fabricated from silicon oxynitride. Waveguide mode dispersion differences between the waveguide modes provide a mechanism for identifying input wavelength shifts that are measured as shifts in the output far-field diffraction image. At visible wavelengths the device can transduce input wavelength changes into phase responses with a sensitivity of $+0.9$ rad/nm. The lower threshold limit of detection for laser output frequency shifts, is 2.2 GHz or 6 pm at a center wavelength of 635 nm. The TE and TM sensitivities to wavelength are approximately equivalent in the device described.**

***Index Terms*—Dispersion, interferometer, optical waveguides, wavelength lockers.**

I. Introduction

DEVICES that can track and stabilize the output wavelength of semiconductor diode lasers are increasingly important as channel count increases in the ITU grid. This task is most commonly served by a discrete microoptical component such as a Fabry–Pérot thin-film filter which acts via photodiodes to provide an error signal to a feedback loop that controls the output frequency of the laser [1], [2]. Alternative methods have been proposed that would allow, in principle, monolithic integration of a control element with wavelength transparent operation [3]. The latter becomes important with the advent of widely tunable laser sources that will enter the marketplace in the next few years [4].

Interferometric detection of wavelength shifts can be an extremely sensitive method, but it has not been explored significantly in the context of diode laser wavelength shifts. The present work describes such a method that also offers the prospect of monolithic integration and wavelength transparent operation.

A. Dual Slab Waveguide Interferometer

We have developed a dual slab waveguide interferometer that provides an output diffraction pattern whose intensity distribution is sensitive to the input wavelength.

The simple fabrication of the interferometer comprises a 5-layer dielectric stack on a semiconductor wafer surface (Fig. 1).

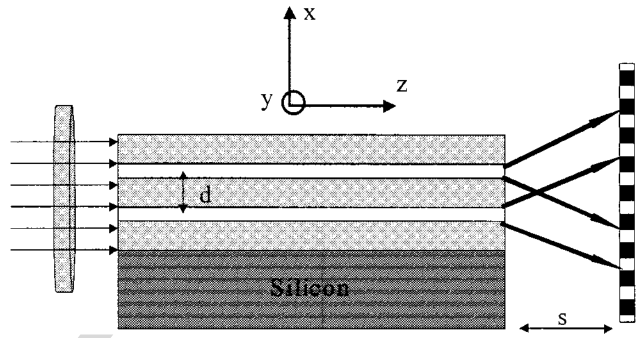

Fig. 1. Dual slab waveguide interferometer. Alternate layers of high (clear) and low (shaded) refractive indexes comprise an interferometer with two separate waveguide paths. A waveguide mode dispersion difference exists between the upper and lower guides when the structure is made structurally or compositionally asymmetric (see text and Table I.

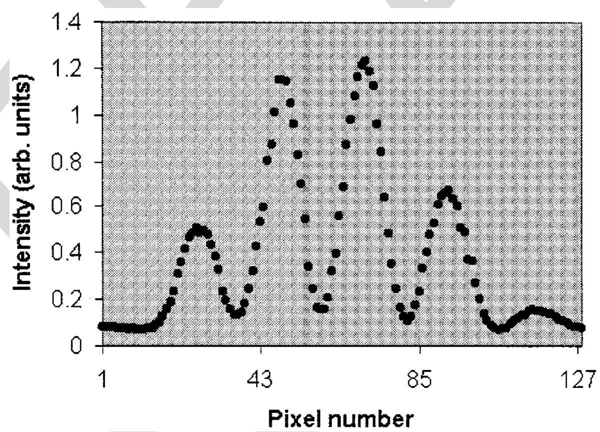

Fig. 2. The interferometer far-field intensity distribution using light at 632.8 nm on a 128-pixel linear photodiode array.

Current devices are fabricated on silicon with silicon oxynitride dielectric layers deposited by PECVD. Since the second and fourth layers are of higher refractive index than their adjacent layers these form optical waveguiding paths, in a dual slab waveguide structure. On introducing an optical field to the entrance plane of the device, the upper and lower modes are excited with equal efficiency and propagate through the structure. At the output plane, the two modes are allowed to diffract into the far field where they form the well-known pattern reminiscent of Young's interference fringes on an array photodiode (Fig. 2). The spatial intensity distribution of the interference pattern is representative of the relative phase position of the output fields of the upper and lower modes at the output plane of the device. Should this change, the spatial intensity distribution changes, thus providing the transduction method.

Manuscript received January 25, 2002; revised March 7, 2002.
The authors are with the University of Durham, Department of Physics, Durham, DH1 3LE U.K. (e-mail: g.h.cross@durham.ac.uk).
Publisher Item Identifier S 1041-1135(02)04804-8.

TABLE I
LAYER STRUCTURE AND OPTOGEOMETRICAL PROPERTIES OF THE INTERFEROMETER.

Layer	Material	RI	Thickness (μm)
1	SiO_xN_y	1.490 - 1.493	1.987 ±0.040
2	SiO_xN_y	1.521 – 1.522	1.008 ±0.020
3	SiO_xN_y	1.479 – 1.481	2.948 ±0.059
4	SiO_xN_y	1.519 – 1.522	0.985 ±0.020
5	SiO_xN_y	1.481 – 1.484	2.019 ±0.040

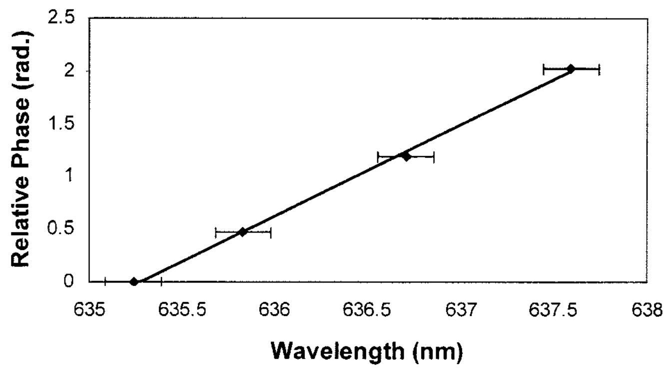

Fig. 3. Sensitivity to wavelength change in TM polarization of an interferometer chip of length $L = 24$ mm.

B. Operating Principles

The guide layer thickness and composition differences gives rise to differences in waveguide mode dispersion between the two guides. Thus, as wavelength changes, the phase retardation produced in the upper ($\Delta\phi_u$) and lower ($\Delta\phi_l$) modal fields differs. The net effect is a phase change difference, Δ, observed between upper and lower waveguide modes according to the following

$$\Delta = |\Delta\phi_u - \Delta\phi_l| = |\Delta\beta_u - \Delta\beta_l| L \tag{1}$$

where L is the interferometer length and $\Delta\beta_{u(l)}$ represents the difference in propagation constant in each mode (upper and lower) due to a wavelength change a to b and given by

$$\Delta\beta_{u(l)} = \left| k_a N^a_{u(l)} - k_b N^b_{u(l)} \right| \tag{2}$$

where $k_{a(b)}$ is the wavenumber, and $N^{a(b)}_{u(l)}$ is the mode effective index in the upper or lower mode, at the two wavelengths a and b. Note that the interferometer returns the sign of Δ, as well as its magnitude thus directly distinguishing between wavelength increases or decreases.

II. EXPERIMENTAL DETAILS

The interferometer layer structure is fabricated according to the nominal design parameters given in Table I. Devices are cleaved from the 100 mm diameter wafer which is supplied presawn into strips 5.8 mm in width and normal to the 100 crystal plane.

The interferometer chip is clamped within a dual stage temperature-controlled housing. Temperature control to better than ± 10 mK is readily achievable in this housing. The input light is provided by a visible laser diode (Coherent VLM2.3–5L, 5 mW, 635 nm) and directed onto the chip end face using a low power microscope eyepiece lens ($\times 1\frac{1}{2}$). The laser is held in its own temperature-controlled housing (single stage). The focused laser beam size is large compared with the vertical separation of the waveguides (4 μm), so that light incident upon the device end facet excites the two modes of the structure with approximately equal efficiency. The output light falls on a 128 element linear photodiode array (Texas Instruments, TSL1401) and the pixel voltages are recorded as the amplitudes of the assigned spatial phase position of each pixel in the spatial period given by the fringe image. A discrete Fourier transform updates the phase position of the pattern every 50 ms and provides a relative phase value. 20 point averaging was used to give a data point every second.

A reference beam is tapped from the beam path and the output power and wavelength position is then independently monitored using an Ocean Optics fiber-optic spectrometer (1200 line grating blazed at 750 nm, 10-μm slits). The wavelength resolution full-width at half-maximum (FWHM) of the spectrometer is to within 0.45 nm. Wavelength measurement was possible to a precision of 0.15 nm, however since the CCD array detector provides 3 pixels within this range. A calibration check was performed using a helium neon laser source (632.8 nm) and a miniature diode-pumped frequency doubled Nd–Yag laser (532.0 nm).

Temperature control of the laser over a temperature range 17 °C–24 °C and wavelength measurement using the spectrometer found a thermooptic coefficient of $+0.2$ nm/K.

III. RESULTS AND DISCUSSION

The sensitivity to a wavelength change over 2 nm in a chip of length 24 mm and in transverse magnetic (TM) excitation is shown in Fig. 3. The solid line represents a linear fit to the data with a slope of $+0.863$ rad/nm.

Precise phase measurements taken at thermal equilibrium at two temperatures (23.67 °C and 20.33 °C) provided a value of the thermooptic coefficient of $+0.017$ rad/K. Given the measured laser thermooptic characteristics (0.2 nm/K) and the interferometer wavelength sensitivity (0.86 rad/nm), we would discriminate the thermal effects on the interferometer from the wavelength shifts that the thermal effect would produce in the laser by a factor of 10. Thus, an attractive feature of this design is the large discrimination between thermal and wavelength dispersive effects.

Dispersion measurements made in Transverse Electric (TE) polarization on a chip of length 25 mm yield a sensitivity of 0.94 rad/nm. The sensitivity per millimeter of interferometer length (0.0375 rad/nm·mm) is almost equal to that for TM polarization (0.0358 rad/nm·mm).

A. Theoretical Analysis

The predicted eigenvalues (propagation constants) for the upper and lower waveguide modes and their dispersion have

TABLE II
LAYER STRUCTURE OF A TYPICAL DOUBLE HETEROJUNCTION LASER DIODE EMITTING AT 1.55 μm. "Q" REPRESENTS THE QUATERNARY COMPOUND SEMICONDUCCTOR, InGaAsP

Layer	Material	RI	Thickness (μm)
1	InP	3.17	∞
2	1.3 μm Q	3.39	0.1
3	1.5 μm Q	3.54	0.2
4	1.3 μm Q	3.39	0.2
5	InP	3.17	1.0
6	1.3 μm Q	3.39	0.5
7	Vacuum	1.00	∞

been obtained. From these we obtain the following expected values for Δ for modes in the wavelength range of interest (635–637 nm):

$$\Delta_{\mathrm{TM}} = +0.008\,05 \quad \text{rad/nm}\cdot\text{mm}$$
$$\Delta_{\mathrm{TE}} = +0.008\,68 \quad \text{rad/nm}\cdot\text{mm}$$

Compared to the measured values ($+0.0358$ rad/nm·mm for TM and $+0.0375$ rad/nm·mm for TE) the calculated values are a factor of around four lower, yet in approximately the same ratio. Furthermore, the sign of the expected response (positive phase shift) agrees with experiment. The discrepancy will be dominated by inaccuracies in the reported thickness and index values limited by the ellipsometric determination. The dispersion difference Δ is extremely sensitive to these parameters. If we assume that the lower guide is at its upper thickness and index limits and the upper guide is at its lower limits, a calculation reveals a value for Δ_{TE} of $+0.0716$ rad/nm·mm. Thus, the experimental value ($\Delta_{\mathrm{TE}} = +0.0358$ rad/nm·mm) falls somewhere within these limits.

As a further indication of projected performance, we have calculated the dispersive properties of an interferometer fabricated using a typical material recipe for double heterojunction buried ridge waveguide lasers. The structural and optical properties are given in Table II. The substrate is assumed to be an InP wafer.

Calculation of the normal modes of this structure at the wavelength boundaries of the "C" band (1525 and 1562 nm) and using equations (1) and (2) gave the following average wavelength dispersion sensitivities

$$\Delta_{\mathrm{TE}} = 0.219 \quad \text{rad/nm}\cdot\text{mm}.$$
$$\Delta_{\mathrm{TM}} = 0.207 \quad \text{rad/nm}\cdot\text{mm}.$$

Thus, for a 5 mm device length, and with a noise floor of ± 1 mrad, the wavelength noise floor limit for TE polarized light would be ± 1 pm.

While in practice, there will be some restrictions on the optogeometrical parameters of the layers that could be used, some optimization is nevertheless possible. If one were to follow the prescriptions given by Veldhuis *et al.* [5] and by Pandraud and Parriaux [6], the two waveguides could be engineered to provide maximum and minimum geometric dispersion, respectively. Such performance enhancement would lessen the impact in practice of manufacturing variability on the value of Δ.

IV. CONCLUSION

A dual slab waveguide interferometer has been fabricated and examined for its wavelength dispersive characteristics. In a temperature regulated environment, phase shift responses are measurable above a noise floor of less than 2 mrad, corresponding to a wavelength noise floor of 2.3 pm in TM polarization and 2.13 pm in TE polarization at center wavelengths around 636 nm. A high sensitivity of the dispersion difference to small variations in waveguide composition is suggested to explain a disagreement between experimental results and theoretical predictions. Nevertheless, theoretical predictions confirm the relative ordering of TM to TE sensitivity and the absolute sign of the observed responses. In the design examined, the thermal sensitivity of the structure has the same sign as the wavelength sensitivity, but is one order of magnitude smaller. Projections to structures consisting of high refractive index layers such as those found in the compound semiconductors suggests that interferometers with picometer level wavelength tracking should be possible. Integrating the device with the laser monolithically would bring advantages in reduced noise, and higher efficiency of excitation of the waveguide modes.

ACKNOWLEDGMENT

The authors would like to thank the National Microelectronics Research Center (NMRC) for sample devices. T. Jackson and C. Moore are especially thanked for their design and assembly of the temperature controlled housings. Permission to use the Fourier transform algorithm for phase calculations was gratefully received from Farfield Sensors Ltd.

REFERENCES

[1] D. M. Adams, C. Gamache, R. Finlay, M. Cyr, K. M. Burt, J. Evans, E. Jamroz, S. Wallace, I. Woods, L. Doran, P. Aycliffe, D. Goodchild, and C. Rogers, "Module-packaged tunable laser and wavelength locker delivering 40 mW of fiber-coupled power on 34 channels," *Electron. Lett.*, vol. 37, pp. 691–693, 2001.

[2] J. E. Johnson, L. J.-P. Ketelsen, D. A. Ackerman, L. Zhang, M. S. Hybertsen, K. G. Glogosvsky, C. W. Lentz, W. A. Asous, C. L. Reynolds, J. M. Geary, K. K. Kamath, C. W. Ebert, M. Park, G. J. Przybylek, R. E. Leibenguth, S. L. Broutin, J. W. Stayt, K. F. Dreyer, L. J. Peticolas, R. L. Hartman, and T. L. Koch, "Fully stabilised electroabsorption-modulated tunable DBR laser transmitter for long-haul optical communications," *IEEE J. Select. Topics Quantum Electron.*, vol. 7, pp. 168–177, Mar.–Apr. 2001.

[3] M. Guy, B. Villeneuve, M. Svilans, M. Tetu, and N. Cyr, "Optical frequency control for DWDM networks using sum-frequency generation in multilayer wave-guides," *IEEE Photon. Technol. Lett.*, vol. 6, pp. 453–456, Mar. 1994.

[4] R. O'Dowd, "Tunable and agile laser transmitter developments for future DWDM optical networks: Toward managed wavelength control and switching," *Photonic Network Communications*, vol. 2, no. 1, pp. 97–103, 2000.

[5] G. J. Veldhuis, O. Parriaux, and P. V. Lambeck, "Normalized analysis for the optimization of geometric wavelength dispersion in three-layer slab waveguides," *Opt. Commun.*, vol. 163, pp. 278–284, 1999.

[6] G. Pandraud and O. Parriaux, "Zero dispersion in step index slab waveguides," *J. Lightwave Technol.*, vol. 17, pp. 2336–2341, Nov. 1999.